Winding-number effect in path-integral simulations

Jianshu Cao
Department of Chemistry, University of Pennsylvania, Philadelphia, Pennsylvania 19104-6323
(Received 14 June 1993)

Path-integral expressions of periodic systems are formulated by introducing the concept of the winding number. Computer simulations and a high-temperature expansion demonstrate the quantum effect of the winding number. We then examine the effects of the winding number on the angular and radial distribution functions in two-dimensional polar coordinates both analytically and numerically.

PACS number(s): 02.70.Lq, 05.30.−d

I. INTRODUCTION

There are many systems which are described by the periodic coordinates or periodic boundary conditions: a finite system with periodic boundary conditions is used to simulate a bulk system [1], the electronic motion in a crystalline solid is intrinsically periodic under the adiabatic assumption because of the lattice structure, and any curvilinear coordinate involves a degree of freedom which is periodic. The path-integral formulation of these systems introduces winding numbers [2]. This paper is devoted to investigate the winding-number effect in path-integral Monte Carlo simulations.

In Sec. II we rewrite the conventional form of path integrals with winding numbers into a computationally convenient expression. A high-temperature expansion derived in Sec. III suggests that the distribution function including winding numbers is smoother than the distribution without winding numbers. And this conclusion is further confirmed by Monte Carlo (MC) simulation results in Sec. VI. The winding-number effect is essentially a quantum phenomenon which helps enhance the tunneling effect in periodic systems.

There have been several simulations for systems with rotational degrees of freedom [3–5]. In the approach of Marx and co-workers, the winding-number distribution is sampled in a primitive MC fashion by introducing a trial move with a change of winding number n to $n-1$ or $n+1$. The difficulties associated with their approach are the low acceptance, unless at extremely low temperatures, and the additional relaxation period after each winding-number jump. The first method proposed in Sec. II treats the winding-number terms as a weighting factor and is thus an efficient algorithm. We also suggest Gaussian sampling for the winding number. The formalism presented in this paper factors the additional kinetic-energy term due to the winding number and thus greatly benefits Monte Carlo simulations and analytical analysis. The focus of the paper is to investigate the effects introduced by winding-number terms. This requires an effective algorithm to sample the subspace designated by the winding number and is difficult to accomplish by the primitive method.

Essentially, the rigid rotator model is a one-dimensional problem. The polar coordinate systems to be studied in Secs. IV and V have two degrees of freedom which have not been well studied by simulations previously. In the case of polar coordinates, the periodicity of the angular part is intrinsic [2,6–8]. We examine the winding-number effect of a two-dimensional harmonic oscillator in Sec. VI and find that the angular distribution is smoother and the radial distribution more populated towards the center. This observation confirms the analytical prediction.

The present paper contains only simple models to demonstrate the quantum effects introduced by the winding-number terms in path integrals. Nevertheless, the analysis and conclusions are general, and the simulation schemes can be applied to more complicated physical systems.

II. THE PERIODIC PATH-INTEGRAL PROPAGATORS

Let us first consider a system having one degree of freedom x which is periodic on the interval $[0,L]$. One such example is a particle constrained to a circle. The Feynman representation of quantum-statistical mechanics gives the general Green's function of the Bloch equation in the form of a functional integral [9],

$$\rho^L(x,x';\beta)=\lim_{P\to\infty}\prod_{i=1}^{i=P}\int_{x=0}^{x=L}dx_i\rho^l(x_i,x_{i+1};\epsilon)\times\langle x|x_1\rangle|_{x_{p+1}=x'}, \tag{2.1}$$

where $\epsilon=\beta/P$ is the reduced Euclidean time. We shall first obtain the explicit expression of short-time propagator for the periodic boundary condition using the Fourier transformation

$$\rho^L(x_i,x_{i+1};\epsilon)=\frac{1}{L}\sum_{l=-\infty}^{\infty}\exp\left\{-\left\{\epsilon\left[\left[\frac{2\pi l}{L}\right]^2\frac{\hbar^2}{2m}+\frac{(V_i+V_{i+1})}{2}\right]\right\}\right\}\times\exp\left[\frac{il(x_i-x_{i+1})2\pi}{L}\right], \tag{2.2}$$

where l is an integer. The Poisson summation leads to the following formula:

$$\rho^L(x,x';\beta)=\lim_{P\to\infty}\prod_{i=1}^{P}\left[\left(\frac{m}{2\pi\hbar^2\epsilon}\right)^{1/2}\times\int_0^L dx_i\sum_{n_i=-\infty}^{\infty}\exp(-\epsilon S_i^{n_i})\right]\times\langle x|x_1\rangle|_{x_{p+1}=x'}\ , \tag{2.3}$$

where we designate an integer n_i for each short-time propagator and where the Euclidean action S_i has the form

$$S_i^{n_i}=\frac{m}{2\epsilon\hbar^2}(x_i-x_{i+1}+n_iL)^2+\epsilon\frac{V_i+V_{i+1}}{2}\ . \tag{2.4}$$

Although the position and potential are only defined in the domain of $[0,L]$, we can simply extend both to the whole axis, which implies a periodic potential, that is,

$$V(x+nL)=V(x)\ . \tag{2.5}$$

We shall redefine the intermediate coordinates as

$$\begin{aligned}x_1&=x_1'\ ,\\ x_2&=x_2'+n_1L\ ,\\ x_3&=x_3'+n_1L+n_2L\ ,\\ x_4&=x_4'+n_1L+n_2L+n_3L\ ,\\ &\vdots\end{aligned} \tag{2.6}$$

Now the limits of the integral can be extended to infinities and the potential part remains the same due to the periodicity of the potential. And thus we obtain the final expression

$$\rho^L(x,x';\beta)=\sum_{n=-\infty}^{\infty}\rho(x,x'+nL;\beta)\ , \tag{2.7}$$

where n is the winding number defined as $n=\sum_{i=1}^{P}n_i$, and ρ is the ordinary path integral defined in the whole space.

It is worthwhile to discuss the physical interpretation of the winding number [10,11]. The Feynman path integral is a summation of all possible paths connecting the initial and final position weighted by e^{-S} where S is the Euclidean action. As we restrict the definition of the coordinate to one cycle of L, the history of paths is ill defined. In order to keep track of a path, we shall extend the coordinates to the whole axis.

However, as we redefine the domain of the coordinate, there are possible paths with different end points which correspond to the same observables. The physical value is taken as $x-[x/L]L$, where [ ] denotes the integer part. These paths can be identified by the winding number n. It is proper to view n as an additional degree of freedom.

The stationary phase approximation allows us to write [2]

$$\rho(x,x';\beta)=\sum_n\left[-\frac{1}{2\pi}\frac{\partial^2 S_{\rm cl}}{\partial x\,\partial x'}\right]^{1/2}e^{-S_{\rm cl}}\ , \tag{2.8}$$

where $S_{\rm cl}(x,x';\beta,n)$ is the classical action along the classical path which circles around n times. (For positive n, the circle is counterclockwise; for negative n, the circle is clockwise.) Therefore, the winding number helps identify the trajectory of a particular path.

At this stage, it is quite straightforward to construct path integrals for some other boundary conditions [12,13]. As an example, a particle confined in a hard wall box,

$$V=\begin{cases}V(x), & 0\le x\le L\\ \infty, & \text{elsewhere}\ .\end{cases} \tag{2.9}$$

The path integral for this system is formulated by inserting the completeness relationship,

$$\delta(x_i-x_{i+1})=\sum_{n=-\infty}^{\infty}\frac{2}{L}\sin\frac{\pi n x_i}{L}\sin\frac{\pi n x_{i+1}}{L}\ . \tag{2.10}$$

After algebraic manipulation, we have the propagator in the box

$$\rho_{\rm box}(x,x';\beta)=\sum_{n=-\infty}^{\infty}[\rho(x,x'+nL;\beta)-\rho(-x,x'+nL;\beta)]\ . \tag{2.11}$$

This form assures that the propagator vanishes when one of the end points is at the boundary. Taking L to be infinity, we obtain a path integral in the half-space.

Recently, we derived a new quantum propagator for hard-sphere cavity systems where a winding number has to be introduced so that contributions from different winding number terms cancel each other at the hard-sphere boundary [14]. In this case, the winding number is interpreted as the number of reflections by the hard-sphere boundary.

We can develop another form of the periodic path-integral propagator which is more practical in performing Monte Carlo simulations. We start from the discretized Feynman path integral with a definite winding number n. The canonical ensemble partition function for a quantum particle is taken to be the trace of the Euclidean time propagator. For this reason, we will simply study the diagonal element. Shifting the coordinate according to

$$x_i'=x_i+\frac{(i-1)}{P}nL \tag{2.12}$$

leads to the action

$$S^n=\frac{P}{2\lambda^2}\sum_{i=1}^{P}(x_i'-x_{i+1}')^2+\frac{n^2L^2}{2\lambda^2}+\beta\sum_{i=1}^{P}V\left[x_i'+\frac{(i-1)}{P}nL\right]\ , \tag{2.13}$$

where λ is the thermal wavelength given by

$$\lambda^2=\frac{\hbar^2\beta}{m}\ . \tag{2.14}$$

And the propagator takes the same form for all n,

$$\rho(x_0,x_0+nL;\beta)=\lim_{P\to\infty} \times\prod_{i=1}^{i=P}\frac{1}{2\pi\lambda^2}\int dx_i' e^{-S^n} \times\langle x_0|x_1'\rangle|_{x_{p+1}'=x_0} . \tag{2.15}$$

Henceforth, we replace x_i' by x_i without causing any confusion.

Obviously, the contribution from the winding number n is characterized by the exponential factor of $\exp(-n^2L^2/2\lambda^2)$ and is important only if the thermal wavelength λ has the same order as the periodic length L.

The new form of S^n suggests an algorithm for Monte Carlo simulations. The configurations are sampled according to the ordinary path-integral propagator e^{-S_0}. All the expectation values are taken as summations of n weighted by $e^{-\Delta S^n}$. Here $\Delta S^n=S_n-S_0$ contains the difference between the potential part and the damping factor $n^2L^2/2\lambda^2$. We can truncate the summation over n for $nL/\lambda\gg 1$.

An alternative Monte Carlo method is suitable for extremely low temperature when the summation of n becomes lengthy. We simply take n as an additional variable sampled from $\exp(-n^2L^2/2\lambda^2)$. The Gaussian width $n_0=\lambda/L$ is so large that we could actually take it as a variable which can be generated from the continuous Gaussian distribution.

Finally, we shall introduce the energy estimators. For a specific n, the virial estimator is

$$\varepsilon_n^V=\frac{1}{\beta}-\frac{n^2L^2}{2\lambda\beta} +\sum_i\frac{1}{2P}(x_i-x_P)\frac{\partial}{\partial x_i}V\left[x_i+\frac{i-1}{P}nL\right] +\frac{1}{P}\sum_i V\left[x_i+\frac{i-1}{P}nL\right] \tag{2.16}$$

and the primitive estimator is

$$\varepsilon_n^P=\frac{P}{2\beta}-\frac{1}{2\lambda^2\beta}\sum_i(x_i-x_{i+1})^2 -\frac{n^2L^2}{2\lambda^2\beta}+\frac{1}{P}\sum_i V\left[x_i+\frac{i-1}{P}nL\right] . \tag{2.17}$$

The total energy is the summation of ϵ_n weighted by $e^{-\Delta S^n}$.

III. HIGH-TEMPERATURE APPROXIMATION

It is possible at this point to present a high-temperature approximation of the periodic path-integral propagator. In the limit $P\to\infty$, we write the continuous limit of Eq. (2.15) as

$$\rho(x,x+nL)=\int_x^x[\mathcal{D}x]e^{-S^n} , \tag{3.1}$$

where the Euclidean action S^n takes the form of

$$S^n=\frac{1}{2\lambda^2}\int_0^1\left|\frac{\partial x}{\partial u}\right|^2du+\frac{n^2L^2}{2\lambda^2} +\beta\int_0^1 V(x(u)+unL)du , \tag{3.2}$$

and the notation

$$\int_{x_i}^{x_f}[\mathcal{D}x]=\lim_{P\to\infty} \times\prod_{i=1}^{P}\left|\frac{1}{2\pi\lambda^2}\right|^{1/2}\int dx_i\langle x_i/x_1\rangle|_{x_{P+1}=x_f} \tag{3.3}$$

represents an integration over all the paths starting at x_i and ending at x_f.

There is a widely used high-temperature approximation which is based on the moment expansion of an average of exponents, that is,

$$\langle e^f\rangle=\exp[\langle f\rangle+\tfrac{1}{2}(\langle f^2\rangle-\langle f\rangle^2)+\cdots] . \tag{3.4}$$

Expanding the path in terms of the Fourier series [15,16],

$$x(u)=x_0+\tilde{x}(u) , \tag{3.5}$$

$$\tilde{x}(u)=\sum_{k=1}^{\infty}a_k\sin(k\pi u) , \tag{3.6}$$

diagonalizes the kinetic-energy part. The first moment of potential is the average potential

$$\langle V\rangle=\left|\frac{1}{2\pi\lambda^2(u)}\right|^{1/2}\int d\tilde{x}(u) \times\exp-\left|\frac{\tilde{x}^2}{2\lambda^2(u)}\right| \times V(x_0+\tilde{x}(u))du \tag{3.7}$$

where the Gaussian width is given by

$$\lambda^2(u)=\lambda^2u(1-u) . \tag{3.8}$$

The above expression gives the lower bound of the high-temperature approximation for $n=0$ [15,17,18].

For $n\neq 0$, though the thermal wavelength is small, the path winds around the period L. This means we have to Fourier analyze the path with respect to period L,

$$\int_0^1 V(x_0+nLu+\tilde{x}(u))du=\int_0^1\sum_{m=0}^{\infty}V^{(m)}(x_0+nLu) \times\frac{\tilde{x}^{(m)}}{m!}du =\int_0^1\sum_{m=0}^{\infty}\sum_{l=-\infty}^{\infty}\tilde{V}_l^{(m)}e^{i2\pi nul} \times\frac{\tilde{x}^{(m)}}{m!}du \tag{3.9}$$

where the Fourier coefficients are

$$\tilde{V}_l^{(m)} = n\int_0^{1/n} V^{(m)}(x_0+nLu)e^{-2\pi nlu}du$$
$$= \int_0^1 V^{(m)}(x_0+Lu')e^{-i2\pi lu'}du' \ . \tag{3.10}$$

We have made use of the periodic property of potential so that there is no dependence on the winding number n.

Again, we take the average of the potential,

$$\langle V\rangle = \int_0^1 \sum_{k=0}^{\infty} \frac{1}{2^k k!} V^{(2k)}(x_0+nLu)[\lambda(u)]^{2k}du$$
$$= \sum_{k=0}^{\infty}\sum_{l=-\infty}^{\infty} \tilde{V}_l^{(2k)}(\lambda)^{2k}K_{nl}^k \tag{3.11}$$

where K_{nl}^k is given by

$$K_{nl}^k = \int_0^1 e^{i2\pi nlu}(u-u^2)^k du \ . \tag{3.12}$$

Let us evaluate K_{nl}^k, for $nl\neq 0$,

$$K_{nl}^0 = 0 \ ,$$
$$K_{nl}^1 = -\frac{2}{(2\pi nl)^2} \ ,$$
$$K_{nl}^2 = -\frac{24}{(2\pi nl)^4} \ ,$$
$$\ldots . \tag{3.13}$$

We work out the expansion to order λ^2 giving

$$\langle V\rangle = \tilde{V}_0 + \tfrac{1}{12}\lambda^2\tilde{V}_0^{(2)} + \frac{\lambda^2}{2n^2}\int_0^1 [V^{(2)}(x_0+Lu')-\tilde{V}_0^{(2)}] \times [u'(1-u')-\tfrac{1}{6}]du' \ , \tag{3.14}$$

where the following identity is employed,

$$\sum_{l=1}^{\infty} \frac{-2}{(2\pi l)^2} 2\cos(2\pi u' l) = u'(1-u')-\tfrac{1}{6} \ , \tag{3.15}$$

and where

$$\tilde{V}_0^k = \int_0^1 V^k(x_0+Lu')du' \tag{3.16}$$

is the spatial average of the potential or its derivative. Whereas $n=0$ is an exception,

$$\langle V\rangle = V(x_0)+\tfrac{1}{12}\lambda^2 V^{(2)}(x_0) \tag{3.17}$$

which can be easily obtained from Eq. (3.7) [17].

It is quite obvious to see the physical implications of this approximation. The effective potential with winding numbers contains two global terms $\tilde{V}_0$ and $\tilde{V}_0^2$. The leading local term in Eq. (3.14) is of the order of $(1/n^2)\lambda^2 L^2 V^{(4)}$, the amplitude of which is much smoother as a function of the position than that of V. So we can draw the conclusion that the effect of winding paths is to reduce the variation in the effective potential. The distribution curve exhibits a smoother or less-structured behavior. A quantum effect such as tunneling will be increased.

IV. TWO-DIMENSIONAL PATH INTEGRALS IN POLAR COORDINATES

Feynman's path-integral representation of quantum-statistical mechanics is generally expressed in the form of a functional integral in Cartesian coordinates. It is a natural extension to formulate path integrals in curvilinear coordinates, particularly in polar coordinates. There have been successful efforts to evaluate the path integral in polar coordinates [6–8]. The purpose of this section is to transform the Cartesian functional integral to the polar functional integral which includes winding numbers explicitly and to examine the effect of winding numbers.

We focus on two-dimensional systems. The propagator in Euclidean time is expressed as

$$\rho(\mathbf{r},\mathbf{r}';\beta) = \int_x^{x'}\mathcal{D}x\int_y^{y'}\mathcal{D}y\, e^{-\epsilon(T_i+V_i)} \ , \tag{4.1}$$

where ϵ is the short-time parameter $\epsilon=\beta/P$, V_i is the potential-energy component, and T_i is the kinetic-energy component.

We decompose the kinetic-energy part of the short-time propagator into Bessel functions and angular harmonics. The distance between two vectors in polar coordinates is

$$(\Delta\mathbf{r})^2 = (x_i-x_{i+1})^2+(y_i-y_{i+1})^2$$
$$= r_i^2+r_{i+1}^2-2r_i r_{i+1}\cos(\Delta\theta) \tag{4.2}$$

where $\Delta\theta=\theta_i-\theta_{i+1}$. The relevant part in the kinetic-energy component is

$$F(\Delta\theta) = e^{a\cos\Delta\theta} \tag{4.3}$$

where $a=(mP/\beta\hbar^2)r_i r_{i+1}$. The familiar expansion of θ leads to

$$F(\Delta\theta) = \sum_{l=-\infty}^{\infty} e^{il\Delta\theta}I_l(a) \ , \tag{4.4}$$

where $I_l(a)$ is the modified Bessel function with imaginary argument. In the limit of $P\to\infty$, we can use the asymptotic form of Bessel functions,

$$\lim_{a\to\infty} I_l(z) = \left[\frac{1}{2\pi a}\right]^{1/2}\exp\left[a-\frac{1}{2a}(l^2-\tfrac{1}{4})\right] \ . \tag{4.5}$$

After a Poisson transformation on integer l, F becomes

$$\lim_{P\to\infty} F(\Delta\theta) = \exp\left[a+\frac{1}{8a}\right]\sum_{n=-\infty}^{\infty} e^{-a(\Delta\theta+2\pi n)^2/2} \ . \tag{4.6}$$

Substitution of the above identity into the kinetic-energy component yields

$$e^{-\epsilon T_i} = \sum_{n_i=-\infty}^{\infty}\exp\left[-\left[\frac{m}{2\hbar^2\epsilon}(r_i-r_{i+1})^2+\frac{m}{2\hbar^2\epsilon}r_i r_{i+1}(\theta_i-\theta_{i+1}+2\pi n_i)^2-\frac{\epsilon\hbar^2}{8mr_i r_{i+1}}\right]\right] \ . \tag{4.7}$$

Now we have obtained the short-time propagator in polar coordinates. Because angle θ is a periodic coordinate with a period of 2π, the same treatment Eq. (2.6) which we utilize to handle the periodic coordinate can be applied here. As the result of the above derivation, we have the final form of the path integral in polar coordinates,

$$\rho(\mathbf{r},\mathbf{r}';\beta)=\sum_{n=-\infty}^{\infty}\lim_{P\to\infty}\times\prod_{P=1}^{\infty}\left[\frac{P}{2\lambda^2}\int_0^{\infty}r_i dr_i\int_{-\infty}^{\infty}d\theta_i e^{-S_i^n}\right]\times\langle\mathbf{r}|\mathbf{r}_1\rangle|_{r_{P+1}=r',\theta_{P+1}=\theta'+2\pi n} \tag{4.8}$$

in which

$$S_i^n=\frac{m}{2\hbar^2\epsilon}(r_i-r_{i+1})^2+\frac{m}{2\hbar^2\epsilon}r_i r_{i+1}(\theta_i-\theta_{i+1})^2+\epsilon\left[\frac{V(\mathbf{r}_i)+V(\mathbf{r}_{i+1})}{2}-\frac{\hbar^2}{8mr_i r_{i+1}}\right]. \tag{4.9}$$

The distinct property of the polar-coordinate path integral derives from the angular part. The fact that angle θ is a periodic coordinate introduces the winding number n. The additional potential term of $-\hbar^2/8mr^2$ is purely a quantum effect [6]. It comes from the expansion of $\cos(\Delta\theta)$ in the kinetic-energy term

$$\cos(\Delta\theta)=1-\tfrac{1}{2}\Delta\theta^2+\tfrac{1}{6}\Delta\theta^4+\cdots \tag{4.10}$$

where the first two terms automatically give the classical correspondence of the kinetic energy, that is, $\Delta x^2+\Delta y^2\to\Delta r^2+r^2\Delta\theta^2$. However, to keep the same order of ϵ in the quantum propagator, a higher-order correction in $\Delta\theta$ is necessary. Actually, a simple estimation gives the right answer [7,8],

$$\langle e^{(r^2m\Delta\theta^4/6\hbar^2\epsilon)}\rangle\approx e^{(mr^2/6\hbar^2\epsilon)\langle(\Delta\theta)^4\rangle}=e^{\hbar^2\epsilon/12mr^2}. \tag{4.11}$$

The quantum term takes the form of an inverse square attraction potential which will cause a divergence in the classical limit. The above derivation is only valid in the limit of $P\to\infty$. This implies that this term should be included only when the number of beads P is large enough to demonstrate the subtle quantum attributes.

V. THE CENTRAL FORCE

The above formula Eq. (4.8) is quite general and can be reduced to the central force path integral after the integration of the angular part is carried out. As the potential is not a function of the angular variable, the angular part can be separated out as

$$G(r_i;\beta)=\sum_{n=-\infty}^{\infty}\prod_{i=1}^{P}\left[\frac{P}{2\pi\lambda^2}\right]^{1/2}r_i\int_0^{2\pi}d\theta_i\exp\left[-\frac{p}{2\lambda^2}r_i r_{i+1}(\theta_i-\theta_{i+1})^2\right]\langle\theta|\theta_1\rangle|_{\theta_{p+1}=\theta'+2n\pi}. \tag{5.1}$$

Let us define a new set of angles,

$$\tilde{\theta}_i=\theta_{i+1}-\theta_i, \tag{5.2}$$

where the index i runs from l to P. Because the two end points are fixed, there must be a constraint on $\tilde{\theta}$,

$$\sum_{i=1}^{i=P}\tilde{\theta}=\Delta\theta+2\pi n, \tag{5.3}$$

where $\Delta\theta=\theta'-\theta$. The change of variables yields

$$G(r_i;\beta)=\sum_{n=-\infty}^{\infty}\prod_{i=1}^{P}\left[\frac{P}{2\pi\lambda^2}\right]^{1/2}r_i\times\int_0^{2\pi}d\tilde{\theta}_i\exp\left[-\frac{p}{2\lambda^2}r_i r_{i+1}\tilde{\theta}_i^2\right]\times\delta\left[\sum_n\tilde{\theta}-\Delta\theta-2\pi n\right] \tag{5.4}$$

where the δ function can be written as

$$\delta\left[\sum_n\tilde{\theta}-\Delta\theta-2\pi n\right]=\frac{1}{2\pi}\int_{-\infty}^{\infty}d\omega e^{i\omega(\sum_n\tilde{\theta}-\Delta\theta-2\pi n)}. \tag{5.5}$$

After performing the angular integrals, we arrive at

$$G(r_i;\beta)=\sum_{l=-\infty}^{\infty}\exp\left[-\sum_i\frac{\beta}{P}\frac{l^2\hbar^2}{2mr_i r_{i+1}}\right]e^{-i\Delta\theta l}\frac{1}{\sqrt{rr'}}. \tag{5.6}$$

And the whole propagator reads as

$$\rho(r,r';\beta)=\sum_{l=-\infty}^{\infty}\frac{1}{\sqrt{rr'}}e^{-i\Delta\theta l}\times\prod_{i=1}^{P}\left[\frac{P}{\lambda^2 2\pi}\right]^{1/2}\int_0^{\infty}dr_i e^{-S^l}\times\langle r|r_1\rangle|_{r_{p+1}=r'}, \tag{5.7}$$

where the action is

$$S^l=\sum_{i=1}^{P}\frac{P}{2\lambda^2}(r_i-r_{i+1})^2+\sum_{i=1}^{P}\frac{\beta}{P}\left[\frac{V(r_i)+V(r_{i+1})}{2}+\frac{\hbar^2(l^2-1/4)}{2mr_i r_{i+1}}\right], \tag{5.8}$$

which is exactly the expression obtained before in another way. The radial part is a path integral with additional

potentials resulting from the angular part. The term $l^2\hbar^2/2mr^2$ is the effective angular momentum potential and l is the quantum number.

We now investigate the radial contribution of each winding number. For a specific n, the angular part is

$$G^n(r_i;\beta)=\frac{1}{2\pi}\int_{-\infty}^{\infty}d\omega\frac{1}{\sqrt{rr'}}e^{-i(\Delta\theta+2\pi n)\omega}\times\exp-\left[\sum_{i=1}^{P}\frac{\beta}{P}\frac{\omega^2\hbar^2}{2mr_ir_{i+1}}\right]. \quad (5.9)$$

It is easy to show that the effective potential appearing in the radial part of the path integral is

$$V_{\text{eff}}^n=(\Delta\theta+2\pi n)^2\frac{\bar{r}^2}{2\lambda^2} \quad (5.10)$$

where $\bar{r}^2$ is defined as

$$\frac{1}{\bar{r}^2}=\frac{1}{P}\sum_{i=1}^{P}\frac{1}{r_i^2}. \quad (5.11)$$

Obviously, as the winding number n increases, the effective potential tends to draw the radial distribution closer to the origin.

It is of interest to generalize the results of two-dimensional polar coordinates to higher-dimensional curvilinear coordinates. For the spherical coordinates the derivation is straightforward.

VI. EXAMPLES

We make a comparison of the result obtained using the ordinary path-integral Monte Carlo and periodic path-integral Monte Carlo with winding numbers. This will demonstrate the importance of including winding numbers in the periodic path integrals. The configurations

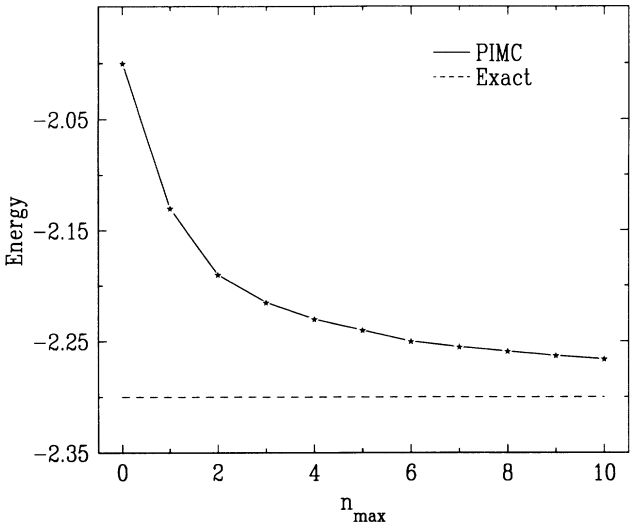

FIG. 2. The same plot as Fig. 1 except for the potential $V=10\cos x$.

are generated by the staging method from e^{-S_0} [19,20]. For a particular winding number n, we shift coordinates according to Eq. (2.12) and weight the configuration by $e^{-(s^n-s^0)}$. The full path integral shall include a summation of the contributions from all the winding-number terms, Eq. (2.7). However in practice, we set a cutoff $n_{\max}$ for the summation of winding numbers, i.e., $-n_{\max}\le n\le n_{\max}$. Terms beyond the cutoff are too small to be counted.

For the sake of simplicity, we choose a cosine potential defined on a circle, $V=V_0\cos(2\pi x)$, $0\le x\le 1$. The

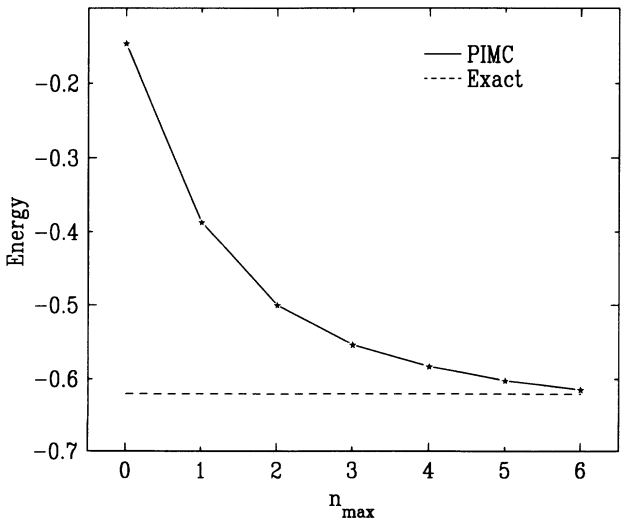

FIG. 1. The average energy E of a quantum particle in potential $V=5\cos x$ as a function of the cutoff $n_{\max}$ in the winding-number summation Eq. (2.7). The dotted line is the exact result.

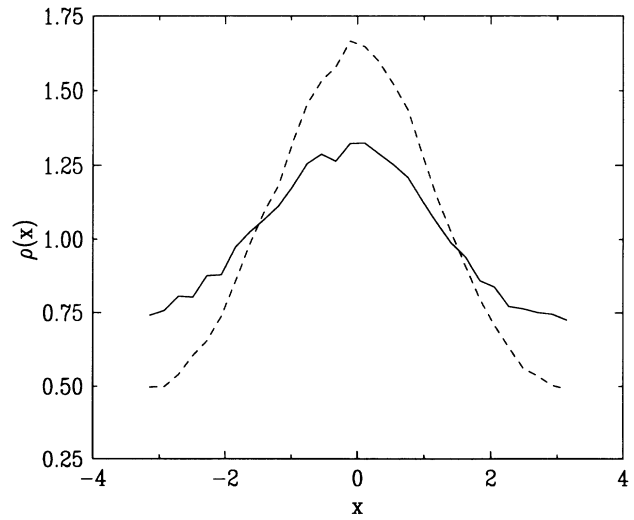

FIG. 3. The distribution function of a quantum particle in potential $V=5\cos x$. The solid curve is the exact result with the winding-number summation. The dashed curve is the result without the winding-number summation.

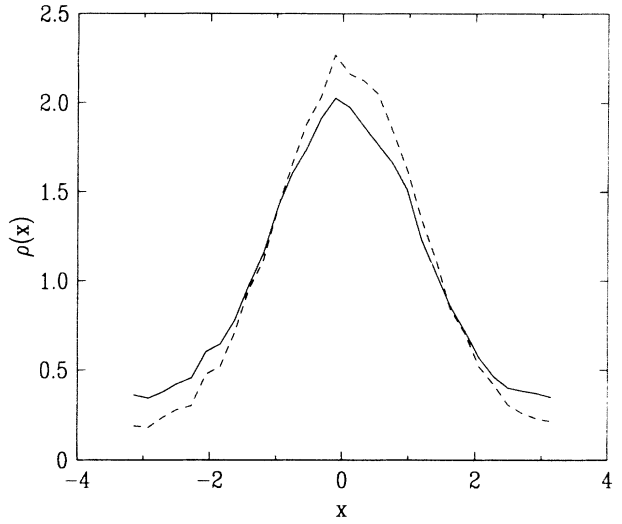

FIG. 4. The same plot as Fig. 3 except for the potential $V=10\cos x$.

relevant constants are taken to be mass$=1.0$, $\hbar=1.0$, $\beta=1.0$. Some trial simulations indicate that a bead number of 30 to 50 is enough to achieve convergence. The number of beads moved in each trial move is adjusted to yield acceptance of about 50%. Data are collected over 10^5 passes.

We plot the average energy E versus the cutoff of the winding-number summation $n_{\max}$. The dotted line is the exact result calculated from the energy eigenvalues solved on a basis set of $e^{i2\pi mx}$. The virial estimator Eq. (2.16) is employed to obtained the average energies: Fig. 1, $V_0=5$; Fig. 2, $V_0=10$. Both curves show the obvious quantum effect of winding numbers. The ordinary path-integral Monte Carlo does not provide the correct energy. As we increase $n_{\max}$, the average energy approaches the value as we expected.

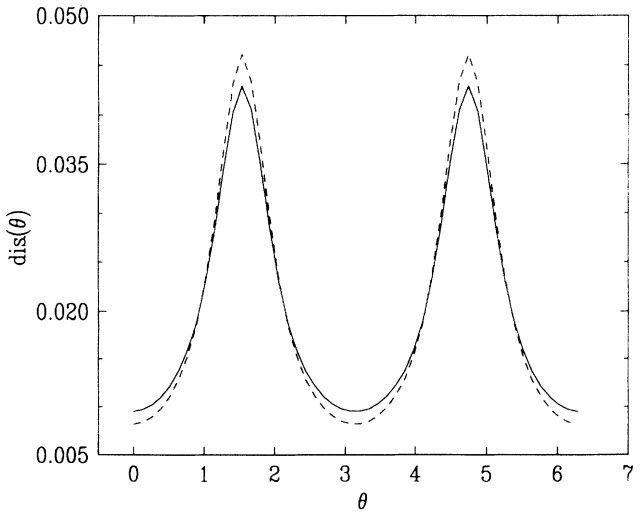

FIG. 5. The angular distribution of a two-dimensional linear harmonic oscillator with frequencies $\omega_x=3.0$ and $\omega_y=1.0$. The solid curve is the exact result and the dashed curve is the result without the winding-number summation.

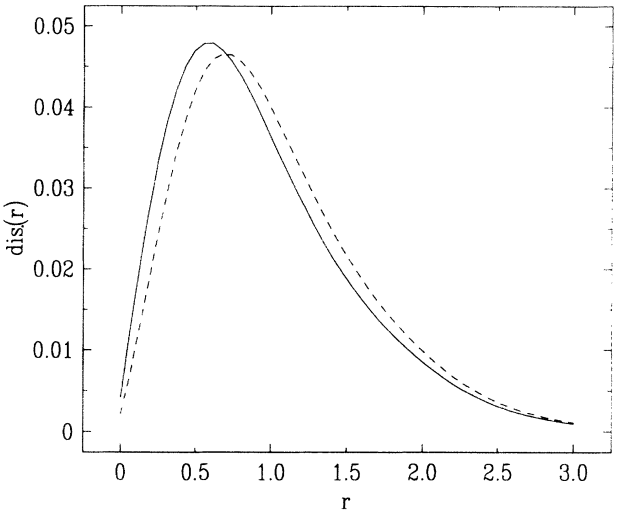

FIG. 6. The radial distribution of a two-dimensional linear harmonic oscillator with frequencies $\omega_x=3.0$ and $\omega_y=1.0$. The solid curve is the exact result and the dashed curve is the result without the winding-number summation.

We also plot the spatial distribution for the same potential. Figure 3 is for the case of $V_0=10.0$; Fig. 4 is for the case of $V_0=5.0$. The solid curve is the distribution after taking the summation over the winding-number terms up to $n_{\max}=10$, which approximates the exact distribution, whereas the dashed curve is for the ordinary path-integral Monte Carlo, which is a special case of the zeroth winding-number term. The fact that the solid curve is smoother than the dashed curve clearly supports our prediction in the previous analysis of the high-temperature approximation [see Eqs. (3.14) and (3.17)]. The nonzero winding-number terms help to increase the quantum tunneling effect.

A two-dimensional linear harmonic oscillator is stud-

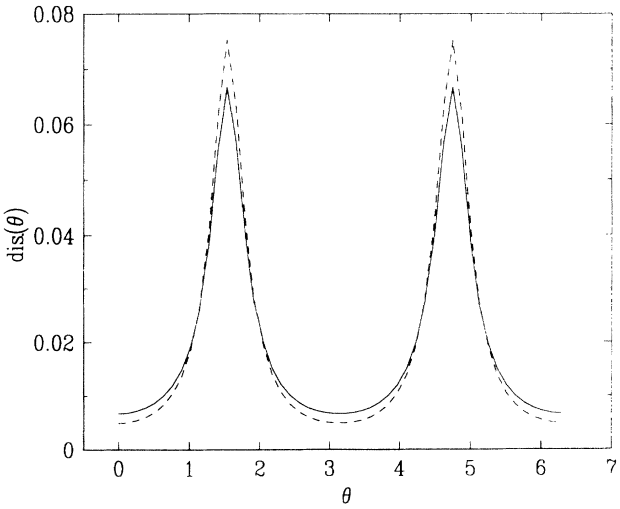

FIG. 7. The same plot as Fig. 5 except for the frequencies $\omega_x=10.0$ and $\omega_y=1.0$.

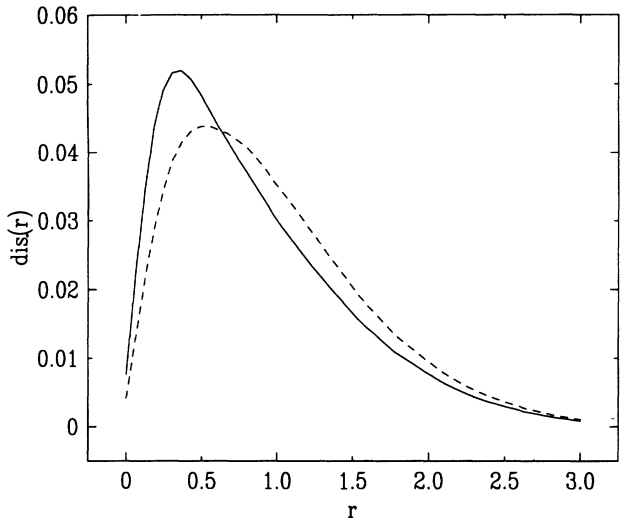

FIG. 8. The same plot as Fig. 6 except for the frequencies $\omega_x = 10.0$ and $\omega_y = 1.0$.

ied to illustrate the winding-number effect in the polar coordinate path integral. The parameters $\hbar$, β, and mass, are set to be one. The potential takes the form of $V = \frac{1}{2}\omega_x^2 x^2 + \frac{1}{2}\omega_y^2 y^2$, in which the ratio of the two frequencies indicates the asymmetry of the potential. Figures 5 and 6 are the radial distribution and the angular distribution, respectively, for the case of $\omega_x = 3.0$, $\omega_y = 1.0$. The solid curve is the distribution of the correct periodic path integral with winding numbers. The dashed curve is the distribution of the ordinary path integral. Figures 7 and 8 are the same plots for the case of $\omega_x = 10.0$, $\omega_y = 1.0$.

We generate configurations of a close chain by the staging Monte Carlo in the Cartesian coordinates. The winding number is calculated for each configuration. Only those with $n = 0$ contribute to the dashed curve. The angular distribution is consistent with our analysis above. And the radial distribution also supports our discussion in Sec. V where we state that the winding-number terms tend to draw the radial distribution towards the origin in the case of central force. This conclusion derived for the central force can be generalized to noncentral force. It can also be noticed that this tendency increases with the asymmetry of the potential.

We have illustrated the quantum aspects of the winding number. Such effects become important for a highly quantized system. As an example, low-temperature hydrogen and its isotopes can be modeled as a system of rigid rotators with weak long-range interactions and strong short-range repulsions. We expect a smoother angular correlation function and a more compact radial correlation function if the winding number is incorporated in the simulations. Moreover, the concept of winding number is essential in formulating the path integral of spin [2] and the propagator for a quantum particle inside a hard cavity [14].

ACKNOWLEDGMENTS

I would like to thank Professor Bruce Berne for many stimulating discussions and encouragement during the course of this work. He introduced me to the field of the path integral and suggested this topic. I also thank Dr. Li (Daohui Li), Dr. Martyna, and Mr. Mishra for reading the manuscript and giving me useful suggestions.

[1] B. J. Berne and D. Thirumalai, Annu. Rev. Phys. Chem. **37**, 401 (1986). For references on the path-integral Monte Carlo method, see the papers cited here.
[2] L. S. Schulman, *Techniques and Applications of Path Integration* (Wiley, New York, 1986).
[3] D. Marx and P. Nielaba, Phys. Rev. A **45**, 8968 (1992).
[4] D. Marx, O. Opitz, P. Nielaba, and K. Binder, Phys. Rev. Lett. **70**, 2908 (1993).
[5] K. J. Runge, M. Surh, C. Mailhiot, and E. L. Pollock, Phys. Rev. Lett. **69**, 3527 (1992).
[6] T. D. Lee, *Particle Physics and Introduction to Field Theory* (Harwood Academic, New York, 1981).
[7] S. F. Edwards and Y. V. Gulyaev, Proc. R. Soc. London Ser. A **279**, 229 (1969).
[8] D. Peak and A. Inomata, J. Math. Phys. **10**, 1422 (1969).
[9] R. P. Feynman and A. R. Hibbs, *Quantum Mechanics and Path Integral* (McGraw-Hill, New York, 1965).
[10] L. S. Schulman, Phys. Rev. **176**, 1558 (1968).
[11] L. S. Schulman, Phys. Rev. **188**, 1139 (1969).
[12] J. A. Barker and M. L. Klein, Phys. Rev. B **7**, 4707 (1973).
[13] J. Barker, J. Chem. Phys. **70**, 3051 (1979).
[14] J. Cao and B. J. Berne, J. Chem. Phys. **97**, 2382 (1992).
[15] R. D. Coalson, D. L. Freeman, and J. D. Doll, J. Chem. Phys. **85**, 4567 (1986).
[16] J. D. Doll, D. L. Freeman, and T. L. Beck, Adv. Chem. Phys. **78**, 61 (1990).
[17] E. P. Wigner, Phys. Rev. **40**, 749 (1932).
[18] N. Makri and W. H. Miller, J. Chem. Phys. **90**, 904 (1989).
[19] M. Spike, M. L. Klein, and D. Chandler, Phys. Rev. B **31**, 4234 (1985).
[20] E. L. Pollock and D. M. Ceperley, Phys. Rev. B **30**, 2555 (1984).